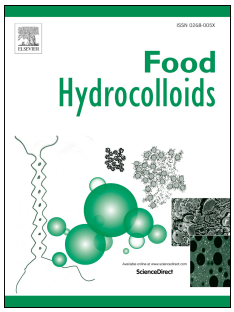

Development of antimicrobial films based on chitosan-polyvinyl alcohol blend enriched with ethyl lauroyl arginate (LAE) for food packaging applications

Hossein Haghighi, Serge Kameni Leugoue, Frank Pfeifer, Heinz Wilhelm Siesler, Fabio Licciardello, Patrizia Fava, Andrea Pulvirenti

PII: S0268-005X(19)31741-2

DOI: https://doi.org/10.1016/j.foodhyd.2019.105419

Reference: FOOHYD 105419

To appear in: *Food Hydrocolloids*

Received Date: 31 July 2019

Revised Date: 2 October 2019

Accepted Date: 2 October 2019

Please cite this article as: Haghighi, H., Leugoue, S.K., Pfeifer, F., Siesler, H.W., Licciardello, F., Fava, P., Pulvirenti, A., Development of antimicrobial films based on chitosan-polyvinyl alcohol blend enriched with ethyl lauroyl arginate (LAE) for food packaging applications, *Food Hydrocolloids* (2019), doi: https://doi.org/10.1016/j.foodhyd.2019.105419.

Chitosan (CS)
(1% w/v)

+

Polyvinyl Alcohol (PVA)
(5% w/v)

CS-PVA Blend FFS
(1:1)

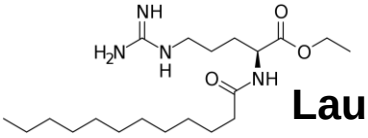

+

Lauroyl Arginate Ethyl (LAE)
(1, 2.5, 5 and 10 % w/w)

CS-PVA-LAE Film

Characterization for Food Packaging Applications

(Microstructure, FT-IR, Thickness, Mechanical, Optical, Water Barrier and Antimicrobial Properties)

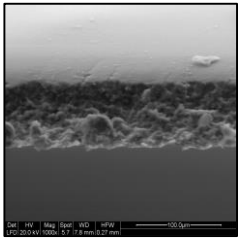

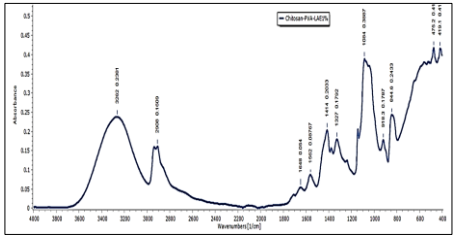

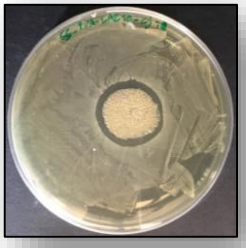

Development of antimicrobial films based on chitosan-polyvinyl alcohol blend enriched with ethyl lauroyl arginate (LAE) for food packaging applications

Hossein Haghighi[a], Serge Kameni Leugoue[a,b], Frank Pfeifer[c], Heinz Wilhelm Siesler[c], Fabio Licciardello[a,d,*], Patrizia Fava[a,d], Andrea Pulvirenti[a,d]

[a] Department of Life Sciences, University of Modena and Reggio Emilia, 42122, Reggio Emilia, Italy

[b] Department of Zootechny, University of Dschang, 222, Dschang, Cameroon

[c] Department of Physical Chemistry, University of Duisburg-Essen, 45117, Essen, Germany

[d] Interdepartmental Research Centre BIOGEST-SITEIA, University of Modena and Reggio Emilia, 42124, Reggio Emilia, Italy

[*] Corresponding author: fabio.licciardello@unimore.it

Abstract

The main aim of this study was to characterize microstructural, physical, optical, mechanical, water barrier and antimicrobial properties of chitosan-polyvinyl alcohol blend films (CS-PVA) enriched with ethyl lauroyl arginate (LAE) (1-10% w/v) for food packaging applications. The film microstructure was determined by scanning electron microscopy. Active films containing 10% LAE showed cracks on the surface with irregular shape in the cross-section indicating a weaker cohesion of the CS-PVA polymer blend at high LAE concentrations. The possible interaction of CS-PVA blend film with incorporated LAE was also investigated using Fourier-transform infrared (FT-IR) spectroscopy in the attenuated total reflection (ATR) mode. FT-IR/ATR spectra showed a low molecular interaction between the CS-PVA and LAE up to 2.5% while for films containing 5 and 10% LAE such interactions between the functional groups of the CS-PVA matrix and LAE have been detected. The active films were transparent and showed barrier properties against UV and visible light. The incorporation of LAE into the CS-PVA increased the thickness, water solubility, water vapor permeability, and the b* and ΔE* values, while it decreased mechanical properties and transparency ($p<0.05$). Active films inhibited the growth of four major food bacterial pathogens including *Campylobacter jejuni*, *Escherichia coli*, *Listeria monocytogenes* and *Salmonella typhimurium*.

Particularly, films containing 5 and 10% LAE were the most effective ($p<0.05$). Overall, the characterization of functional properties revealed that CS-PVA blend film incorporated with LAE could be used as an environmentally friendly antimicrobial packaging material to extend the shelf life of food products.

Keywords: Active food packaging, ATR/FT-IR, Bio-based packaging, Ethyl lauroyl arginate (LAE)

1. Introduction

The current trend in food packaging is mainly oriented towards the substitution of non-biodegradable petroleum-based polymers by packaging materials that are eco-friendly and also prolong food shelf life (Kanatt, Rao, Chawla, & Sharma, 2012). In this context, considerable research has been conducted involving the fabrication of biodegradable food packaging materials that come from renewable natural resources and agri-food industry wastes (Cazón, Vázquez, & Velazquez, 2018; Sarwar, Niazi, Jahan, Ahmad, & Hussain, 2018). Among bio-based natural polymers, chitosan (CS) has received significant attention for its potential to substitute - partially or totally - petroleum-based polymers (Leceta, Guerrero, & De La Caba, 2013). CS is a cationic linear polysaccharide consisting of poly-β-(1–4)-D-glucosamine units obtained by partial deacetylation of chitin, the major component of the insect's exoskeleton and shells of crustacean such as crab, shrimp, and crawfish. CS is the second most abundant polysaccharide after cellulose with unique biological properties such as biocompatibility, biodegradability and non-toxicity. In addition, this amino polysaccharide has high antimicrobial activity against many pathogenic and spoilage microorganisms, including both Gram-positive and Gram-negative bacteria which makes it an excellent candidate for food packaging applications (Rubilar, Candia, Cobos, Díaz, & Pedreschi, 2016). However, there are some limitations which are associated with CS such as low mechanical strength, low thermal stability, rigid crystalline structure and high production cost. A simple and effective alternative to overcome these drawbacks could be blending of CS with synthetic polymers. Films formed by the blending of natural and synthetic polymers represent a new class of material with modified physical and mechanical properties

compared to films made of individual components. Blending CS with polyvinyl alcohol (PVA) has been intensively investigated by many researchers to gain biodegradable and antimicrobial films for food packaging applications with new and desired properties (Bonilla, Fortunati, Atarés, Chiralt, & Kenny, 2014; Kanatt et al., 2012; Liu, Wang, & Lan, 2018; Tripathi, Mehrotra, & Dutta, 2009; Parida, Nayak, Binhani, & Nayak, 2011).

PVA is a synthetic, low cost, non-toxic and water-soluble polymer commercially obtainable from hydrolysis of polyvinyl acetate with excellent film forming properties. Despite its synthetic character, this polymer was recognized as biodegradable and it shows high tensile strength, flexibility, gas barrier properties and good resistance to acid and alkali media (Aloui et al., 2016). PVA has been evaluated for safety by the Joint FAO/WHO Expert Committee on Food Additives (JECFA) in 2003 at the 61st meeting (Bellelli, Licciardello, Pulvirenti, & Fava, 2018) and it has also been approved for use in packaging meat and poultry products by the USDA (Kanatt et al., 2012). PVA is highly miscible with other hydrophilic polymers such as CS, owing to the formation of intermolecular hydrogen bonds between hydroxyl groups of PVA and hydroxyl and amine groups of CS. Due to the high compatibility of CS and PVA, the resulting films show homogeneous structure. Moreover, blending PVA with CS is a promising strategy to reduce the production cost and improve the mechanical property and stability of CS films.

Antimicrobial packaging as a part of active packaging systems is intended to extend the shelf life of food products and assure the safety and quality of packaged foods (Tripathi, Mehrotra, & Dutta, 2008). Ethyl lauroyl arginate (LAE) is considered as an effective antimicrobial substance among novel food additives (Rubilar et al., 2016). LAE remains stable at pH 3-7 and is odorless and colorless as well (Kashiri et al., 2016). LAE is a synthetic surfactant consisting of an ethyl esterified arginine head with a lauroyl tail attached to the α-amino group that is highly active against a wide range of food pathogens and spoilage microorganisms including bacteria, yeast and molds with a low-dose application (Becerril, Manso, Nerin, & Gómez-Lus, 2013). This cationic surfactant disrupts the cytoplasmic membrane of microorganisms and inhibits the growth of microorganisms by causing cell

deformation and affecting their metabolic process negatively (Muriel-Galet, Carballo, Hernández-Muñoz, & Gavara, 2016). LAE has been considered as GRAS (generally recognized as safe) by the U.S. Food and Drug Administration (FDA, 2005) and has been authorized as food preservative by the European Food Safety Authority (EFSA, 2007). Incorporation of LAE as an antimicrobial compound into antimicrobial packaging to improve food safety and quality has been reported in several studies (De Leo et al., 2018; Haghighi et al., 2019a; Higueras, López-Carballo, Hernández-Muñoz, Gavara, & Rollini, 2013; Kashiri et al., 2016; Moreno, Cárdenas, Atarés, & Chiralt, 2017a; Rubilar et al., 2016). However, literature concerning the effects of LAE on the functional properties of CS-PVA blend film is not available. Therefore, the objective of the present study was to develop biodegradable films based on CS-PVA blend enriched with different concentrations of LAE to evaluate microstructural, physical, optical, mechanical and water barrier properties for food packaging applications. Moreover, the antimicrobial activity of films against four common food bacterial pathogens including *Campylobacter jejuni*, *Escherichia coli*, *Listeria monocytogenes* and *Salmonella typhimurium,* was investigated.

2. Material and methods

2.1 Materials and reagents

Chitosan (CS) with a molecular weight of 100-300 kDa was obtained from Acros Organics™ (China). Polyvinyl alcohol (PVA) with molecular weight of 27 kDa and 98% degree of hydrolysis was purchased from Fluka (Steinheim, Germany). Glycerol (≥ 99.5%) was purchased from Merck (Darmstadt, Germany). Acetic acid (≥ 99.5%) was obtained from Brenntag S.p.A (Milan, Italy). Ethyl lauroyl arginate (LAE) was kindly provided as Mirenat-D (69.3% LAE, 30.7% maltodextrin) by Vedeqsa Grupo LAMIRSA (Terrassa, Barcelona, Spain). Brain heart infusion agar (BHIA) was purchased from Biolife (Milan, Italy).

2.2. Preparation of film-forming solutions (FFS) and films

Preparation of films was adapted from the procedures of Higueras et al., (2013) and Kanatt et al., (2012) with slight modification. In this study, four CS-PVA blend films enriched with different concentrations of LAE (1, 2.5, 5 and 10% w/w of biopolymer) were analyzed.

Furthermore, a CS-PVA film-forming solution (FFS) without LAE was used to produce a control film. The CS FFS (1%, w/w) was prepared by dissolving CS in an acetic acid solution (1% v/v) under continuous stirring at 55°C for 60 min. The PVA FFS (5% w/w) was prepared by dissolving PVA in distilled water at 80°C for 60 min. Glycerol (0.5% v/v of FFS) was then added as a plasticizer into both FFSs, followed by additional stirring for 60 min. The CS-PVA blend FFS was prepared by mixing CS and PVA FFSs at 1:1 ratio and final plasticizer content was 17g glycerol/ 100 g dry polymer. Different amounts of LAE were added to the CS-PVA blend FFS to obtain active films with 1-10% LAE (g of LAE/100 g of dry CS-PVA blend) considering the LAE concentration (69.3%) in Mirenat-D. All FFSs were degasified with a vacuum pump (70 kPa) for 15 min to remove bubbles. Films were obtained by casting 20 mL of the FFS into Petri dishes (14.4 cm in diameter) and drying at 25±2 °C in the chemical hood overnight.

2.3. Scanning electron microscopy (SEM)

The SEM images from the surface and cross-section of the films were obtained with the use of a scanning electron microscope (FEI, Quanta 200, Oregon, USA). Film samples were fixed on a stainless-steel support with a double-sided conductive adhesive. The analysis was conducted in low vacuum (0.6 Torr) at an acceleration voltage of 20 kV.

2.4. Atomic force microscopy (AFM)

The surface morphology of the films was analyzed using an atomic force microscope (Park Scientific Instruments, South Korea). Films were fixed onto AFM specimen metal discs using a double-sided tape and then placed to a magnetic sample holder located on the top of the scanner tube. The images were scanned in no-contact mode under ambient condition. The surface roughness (R_a) of the films was calculated on the basis of the root mean square (R_q) deviation from the average height of peaks after subtracting the background using ProScan software (version 1.51b). All samples were analyzed in triplicate.

2.5 Attenuated Total Reflection (ATR) / Fourier-Transform Infrared (FT-IR) Spectroscopy

The infrared spectra of different films were obtained using an ATR/FT-IR spectrometer (type Alpha, Bruker Optik GmbH, Ettlingen, Germany). Spectra were collected from two different locations from the top and bottom side of the same samples in the 4000-400 cm^{-1} wavenumber range by accumulating 64 scans with a spectral resolution of 4 cm^{-1}.

2.6. Thickness and mechanical properties

Film thickness was measured with a digital micrometer (Model IP65, SAMA Tools, Viareggio, Italia) at five different random positions (one at the center and four at the edges). The means of these five separate measurements were recorded.

The tensile strength (TS), elongation at break (E%) and elastic modulus (EM) were determined using a dynamometer (Z1.0, Zwick/Roell, Ulm, Germany) according to ASTM standard method D882 (ASTM, 2001a). The films with known thickness were cut into rectangular strips (9.0 x 1.5 cm^2). Initial grip separation and cross-head speed were set at 70 mm and 50 mm/min, respectively. Measurements were repeated 10 times from each type of film. The software TestXpert® II (V3.31) (Zwick/Roell, Ulm, Germany) was used to record the TS curves. TS was calculated by dividing the maximum load to break the film by the cross-sectional area of the film and expressed in MPa. The E% was calculated by dividing film elongation at rupture by the initial grip separation expressed in percentage (%). EM was calculated from the initial slope of the stress-strain curve and expressed in MPa.

2.7. UV barrier, light transmittance, opacity value and color

The barrier properties of films against UV and visible light were determined at the UV (200, 280 and 350 nm) and visible (400, 500, 600, 700 and 800 nm) wavelengths. These optical characteristics were estimated with a VWR®Double Beam UV-VIS 6300PC spectrophotometer (China) using square film samples (2 × 2 cm^2). The opacity of the films was calculated by Eq. (1):

$$\text{Opacity value} = \frac{-\log T_{600}}{x} \quad (1)$$

where T_{600} is the fractional transmittance at 600 nm and x is the film thickness (mm). The greater opacity value represents the lower transparency of the film. For each film, four readings were taken at different positions and average values were determined.

The color of films was measured with a CR-400 Minolta colorimeter (Minolta Camera, Co., Ltd., Osaka, Japan) at room temperature, with D65 illuminant and 10° observer angle. The instrument was calibrated with a white standard (L* = 99.36, a* = -0.12, b* = -0.07) before measurements. Results were expressed as L* (lightness), a* (red/green) and b* (yellow/blue) parameters. The total color difference (ΔE^*) was calculated using the following Eq. (2):

$$\Delta E^* = \sqrt{[(\Delta L^*)^2 + (\Delta a^*)^2 + (\Delta b^*)^2]} \quad (2)$$

where ΔL^*, Δa^* and Δb^* are the differences between the corresponding color parameter of the samples and that of a standard white plate used as the film background. For each film, five readings were taken at different positions and the average values were determined from the top and bottom sides.

2.8. Moisture content and water solubility

Moisture content (MC) of the films (2 × 2 cm^2) was determined as the percentage of weight loss upon drying to constant weight (Md) in an oven at 105 ± 2 °C and the initial weight (Mw) according to the following Eq. (3):

$$\text{MC (\%)}: \frac{Mw - Md}{Mw} \times 100 \quad (3)$$

The solubility of films (2 × 2 cm^2) in water was determined by drying to constant weight in an air-circulating oven at 105± 2 °C (Wi) and then each film was immersed in 50 mL distilled water at 25 °C following Gontard, Guilbert, & Cuq, (1992) with slight modifications. After 24 h, the film samples were dripped and dried to constant weight at 105± 2 °C (Wf) to determine the weight of dry matter which was not solubilized in water. The measurement of water solubility (WS) was determined according to the following Eq. (4):

$$\text{WS (\%)}: \frac{Wi - Wf}{Wi} \times 100 \quad (4)$$

All measurements for MC and WS were made in triplicate.

2.9. Water vapor transmission rate and water vapor permeability

Water vapor transmission rate (WVTR) of the films was determined gravimetrically in triplicate according to the ASTM E96 method (ASTM, 2001b) with some modifications. Films were sealed on top of glass test cups with an internal diameter of 10 mm and a depth of 55

mm filled with 2 g anhydrous $CaCl_2$ (0% RH). The cups were placed in desiccators containing $BaCl_2$ (90% RH), which were maintained in incubators at 45 °C. WVTR was determined using the weight gain of the cups and was recorded and plotted as a function of time. Cups were weighed daily for 7 days to guarantee the steady state permeation. The slope of the mass gain versus time was obtained by linear regression ($r^2 \geq 0.99$). WVTR (g /day m^2) and WVP (g mm/kPa day m^2) were calculated according to the following Eqs. (5) and (6):

$$WVTR = \frac{\Delta W}{\Delta t \times A} \quad (5)$$

$$WVP = \frac{WVTR \times L}{\Delta P} \quad (6)$$

where $\Delta W/\Delta t$ is the weight gain as a function of time (g/day), A is the area of the exposed film surface (m^2), L is the mean film thickness (mm) and ΔP is the difference of vapor pressure across the film (kPa).

2.10. In vitro antimicrobial activity

2.10.1. Disk diffusion assay

Antibacterial activity test on films was assessed against four typical food bacterial pathogens including *Listeria monocytogenes* (UNIMORE 19115), *Escherichia coli* (UNIMORE 40522), *Salmonella typhimurium* (UNIMORE 14028) and *Campylobacter jejuni* (UNIMORE 33250) using the disk diffusion assay according to (Haghighi et al., 2019). Films (sterilized with UV light) were cut into a disc shape of 22 mm diameter and placed on the surface of BHIA agar plates, which had been previously streaked with 0.1 mL of inocula containing 10^6 CFU/mL of tested bacteria. The plates were then incubated at 30 °C for 24 h (*C. jejuni* plates were incubated at 37 °C). The diameter of the inhibition zones was measured with a caliper and recorded in millimeters (mm). All tests were performed in triplicates.

2.10.2. Evaluation of antimicrobial activity in liquid medium

Antimicrobial activity of CS-PVA films enriched with LAE (1-10%) evaluated against *L. monocytogenes*, *E. coli*, *S. typhimurium* and *C. jejuni* in liquid medium (Kashiri et al., 2016). A loop of each strain was transferred to 10 mL of BHIB and incubated at 30°C (*C. jejuni* plates were incubated at 37 °C) for 24 h to obtain stationary phase (optical density of 0.9 at 600 nm). Then, cells were diluted in BHIB and incubated at 30 °C (*C. jejuni* tube was

incubated at 37 °C) to obtain exponential phase (optical density of 0.2 at 600 nm). One hundred µL of microorganism in exponential phase was inoculated into tubes with 10 mL of BHIB. A 0.025 g portion of film (1.5 x 1.5 cm^2) was added to each tube in sterile conditions. The tubes were incubated at 30°C for 24 h. As a control, CS-PVA film without LAE was used. Depending on the turbidity of each tubes, serial dilutions with NaCL were made and plated on the Petri dishes with BHIA culture medium. Colonies were counted after incubation at 30 °C for 24 h.

2.10. Statistical analysis

The statistical analysis of the data was performed through analysis of variance (ANOVA) using SPSS statistical program (SPSS 20 for Windows, SPSS INC., IBM, New York). The experiment was performed in 3 replicates and the number of repeats varied from one analysis to another and was reported in each subsection. The differences between means were evaluated by Tukey's multiple range test ($p<0.05$). The data were expressed as the mean ± SD (standard deviation).

3. Results and discussion

3.1. Scanning electron microscopy (SEM)

The surface and cross-section images of CS-PVA blend film (control) and CS-PVA film enriched with different concentrations of LAE (1-10%) (active films) are presented in Fig. 1. The film microstructure greatly affects the final physical, mechanical and barrier properties. This is mainly due to the interaction between the film components and LAE. The surface of the control film was smooth and homogenous and did not show pores or cracks indicating good compatibility between CS and PVA to form a blend (Fig. 1a). This could be explained by strong molecular interaction between functional groups of chitosan and PVA. Similar results were reported by Ghaderi, Hosseini, & Gómez-Guillén (2019) and Jahan, Mathad, & Farheen (2016) who noticed that the surface of CS-PVA blend film was homogenous without pores. Addition of LAE up to 1% did not affect the surface morphology of active films (Fig. 1c) indicating LAE was evenly distributed and well dispersed in the film matrix. Small particles and aggregations were observed at the surface of films with increasing concentration of LAE

up to 10% (Fig. 1e, 1g and 1i). A compact and continuous structure without irregularities like air bubbles and pores and any evidence of phase separation can be observed in the cross-section of the control film (Fig. 1b). The cross-section of active films containing LAE up to 2.5% showed similar results (Fig. 1d and 1f). However, active films containing 5 and10% LAE showed irregular and sponge shape structure (Fig. 1h and 1j). This effect was more obvious in CS-PVA film containing 10% LAE. This might be related to the agglomeration of LAE in the film matrix at high concentrations which resulted in disrupted structures. The interaction between the polymer chains was disturbed by interactions with functional groups of LAE, producing films with less integrity. Gaikwad, Lee, Lee, & Lee (2017) also reported that the order of low-density polyethylene (LDPE) films was interrupted by the addition of high amount of LAE powder (5 and 10%) mainly due to the inhomogeneous distribution of LAE inside the matrix and the low interfacial interaction between the LDPE and LAE powder.

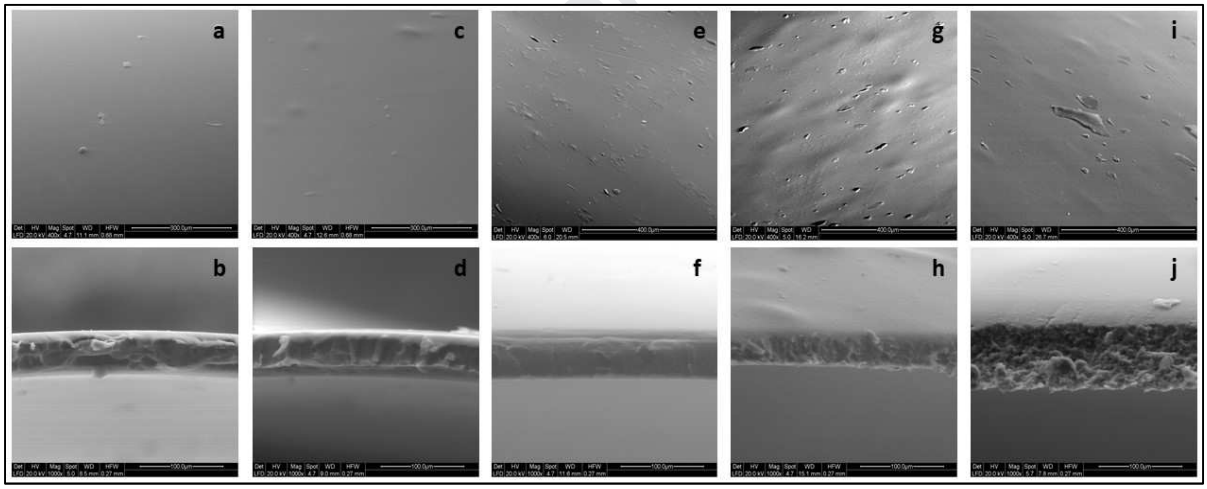

Fig. 1. Scanning electron microscopy (SEM) images of the surface and cross-section of films based on a control CS-PVA blend (CS-PVA) (a and b), CS-PVA-LAE1% (c and d), CS-PVA-LAE2.5% (e and f), CS-PVA-LAE5% (g and h) and CS-PVA-LAE10% (i and j).

3.2. Atomic force microscopy (AFM)

AFM was further performed to characterize the surface morphology of control and active films. Typical 3D surface topographic AFM images and root mean square (R_q) and roughness (R_a) values are presented in Fig. 2. The surface of control film was relatively smooth and homogenous as indicated by lower R_q and R_a values (17.1 and 12.0 nm, respectively). Increasing concentration of LAE up to 10% led to the increase in the roughness of the films, as indicated by higher R_q and R_a values. The difference in roughness

value between control and active films was in accordance with the film microstructure observed by SEM analysis.

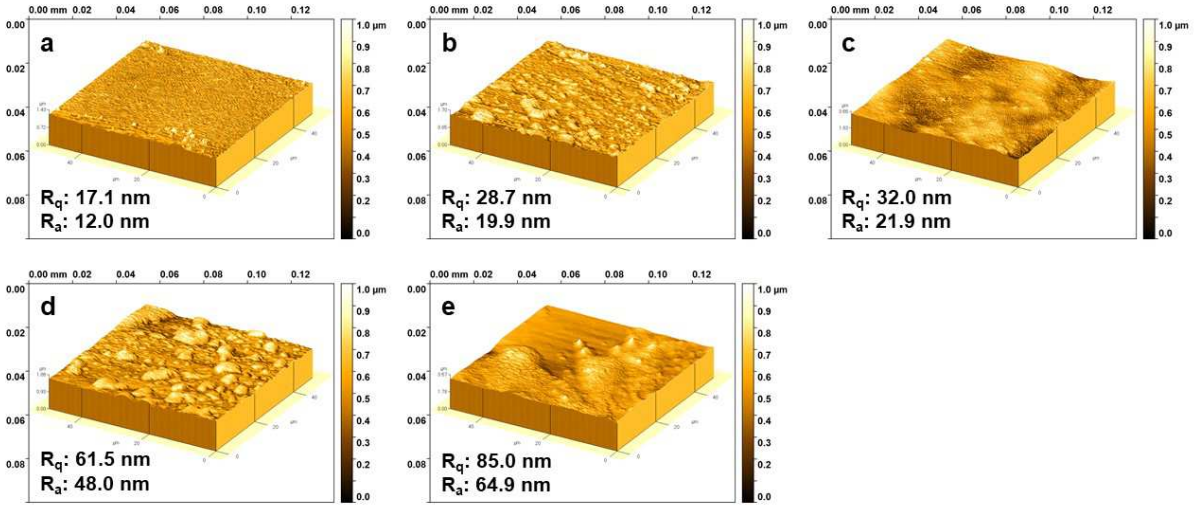

Fig. 2. 3D AFM images, root mean square (R_q) and roughness (R_a) of films based on a: control CS-PVA blend, b: CS-PVA-LAE 1%, c: CS-PVA-LAE 2.5%, d: CS-PVA-LAE 5% and e: CS-PVA-LAE 10%.

3.3. Attenuated Total Reflection (ATR) / Fourier-Transform Infrared (FT-IR) Spectroscopy

ATR/FT-IR spectroscopy was performed to characterize the structural and spectroscopic changes due to the incorporation of different amounts of LAE (1-10% w/w) into the CS-PVA film matrix by measuring the spectra in the wavenumber range of 4000-400 cm^{-1} at a spectral resolution of 4 cm^{-1}. The spectrum of the control CS-PVA blend (Fig. 3A, a) revealed the characteristic bands of the two polymer components (CS and PVA) with relative intensities according to the respective composition. Under the broad and intense absorption band with the maximum at about 3270 cm^{-1}, the ν(OH), ν(NH) and $\nu_{as}(NH_2)/\nu_s(NH_2)$ absorption bands of these inter- and intramolecularly hydrogen bonded functionality of the CS and PVA blend components are superimposed (Costa-junior, Pereira, & Mansur, 2009; Kumar, Krishnakumar, Sobral, & Koh, 2019). The neighboring band doublet at about 2937/2908 cm^{-1} can be assigned to antisymmetric and symmetric $\nu_{as}(CH_2)/\nu_s(CH_2)$ and ν(CH) stretching vibrations of the corresponding polymer chain functionalities (Liu et al., 2018). Characteristic absorption bands for CS can be assigned at 1646 cm^{-1} (amide-I) due to

the ν(C=O) stretching vibration, and at 1561 cm^{-1} (amide II) to a combination band of the ν(C–N) stretching and δ(N-H) bending vibrations (Costa-junior et al., 2009). Because in this study a PVA with only 98% degree of hydrolysis was used, 2% of acetate groups remained non-hydrolyzed during the manufacturing process (Koosha & Mirzadeh, 2015). Thus, the band at 1708 cm^{-1} belongs to the ν(C=O) stretching vibration of residual vinyl acetate units in the PVA backbone (Costa-junior et al., 2009). The very sharp, crystallinity-sensitive band of PVA at 1140 cm^{-1} is also observed in the CS-PVA blend (Kim, Kim, Lee, & Kim, 1992; Tripathi et al., 2009). Furthermore, absorption bands at 1413 cm^{-1} (δ(CH_2) bending vibration), between 1085 and 1045 cm^{-1} (ν(C–O) stretching vibrations), and 917 cm^{-1} (CH_2 rocking vibration) can be observed in the ATR/FT-IR spectrum of the CS-PVA blend (Pavaloiu, Stoica-Guzun, Stroescu, Jinga, & Dobre, 2014; Pereira Jr, de Arruda, & Stefani, 2015). For a better visualization and understanding of the – although minor – spectral changes in the wavenumber ranges 2800 – 3000 cm^{-1} and specifically 1500 – 1800 cm^{-1} (see Fig. 3B) upon addition of LAE to the CS-PVA blends, the spectrum of pure Mirenat-D is reproduced in Fig.4. The most important absorption bands of the spectral range between 1000 and 3500 cm^{-1} can be readily assigned to the different vibrations of the chemical building blocks of this additive.

Up to 2.5% LAE content, the characteristic absorption bands in the ATR/FT-IR spectra of the CS-PVA blends (Fig. 3A, b and c) are wavenumber invariant and do not show intensity changes, thereby suggesting low molecular interaction between the polymer and the LAE. Similar results were reported by Gaikwad, Lee, Lee, & Lee (2017); Rubilar et al. (2016) and Kashiri et al. (2016). However, CS-PVA blend films containing 5% and 10% LAE (Fig. 3A, d and e) revealed new absorption bands at 2918 cm^{-1} and 2851 cm^{-1} ($\nu_{as}(CH_2)/\nu_s(CH_2)$), 1755 cm^{-1} (ν(C=O)), 1724 cm^{-1} (ν(C=O)) and 1661/1645 cm^{-1} (ν(C=O), ν(C=N), δ(NH_2)) originating from the introduction of new CH_2-segments, ester, amide, NH_2 and imine groups (Gamarra, Missagia, Urpí, Morató, & Muñoz-Guerra, 2018; Moreno et al., 2017a). The evolution of the band doublet (1661/1645 cm^{-1}) from the original 1646 cm^{-1} band and the shift of the 1561 cm^{-1} band to 1557 cm^{-1} (LAE 5%) and to 1544 cm^{-1} (LAE 10%), respectively (Fig. 3B, d and e), is

a clear evidence, that at elevated LAE content the C=O, NH_2 and NH functionalities of this additive contribute to competitive intermolecular interactions with the hydroxyl, amino, ether and residual acetate groups of the CS-PVA film network. Furthermore, LAE can also promote the formation of C=N groups, by reacting with both, residual acetate carbonyls of PVA and CS amino groups, as revealed by the relative intensity of the peak at 1645 cm^{-1} for LAE 10% (Fig 3B, e). Thus, the carbonyl-amino reaction to form C=N groups was enhanced by the presence of LAE (Moreno et al., 2017a).

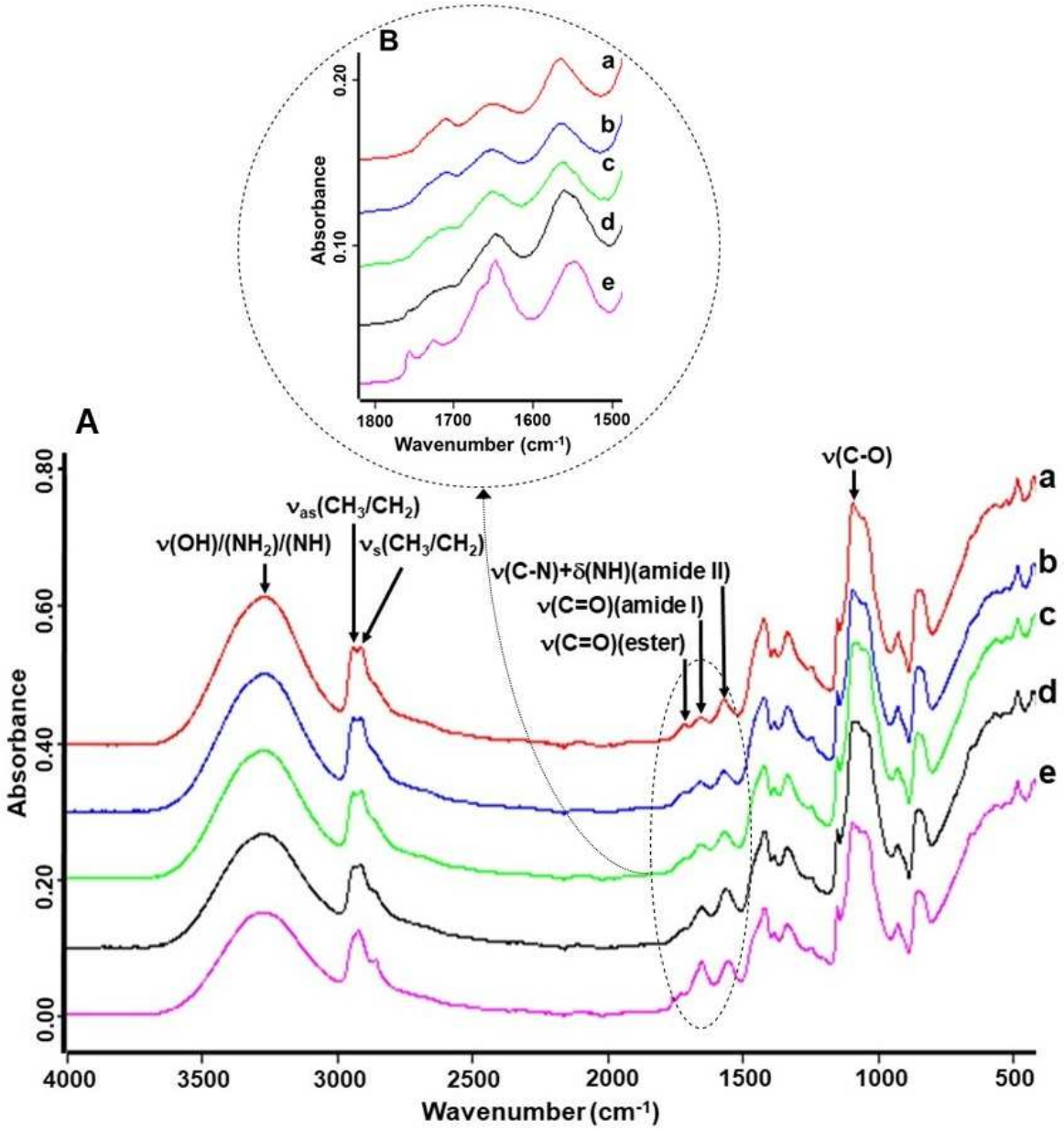

Fig. 3. ATR/FT-IR spectra (A) of films based on a: control CS-PVA blend, b: CS-PVA-LAE 1%, c: CS-PVA-LAE 2.5%, d: CS-PVA-LAE 5% films and e: CS-PVA-LAE 10%. In (B) the enlarged 1800-1500 cm^{-1} region is shown to highlight the spectral changes at elevated LAE content.

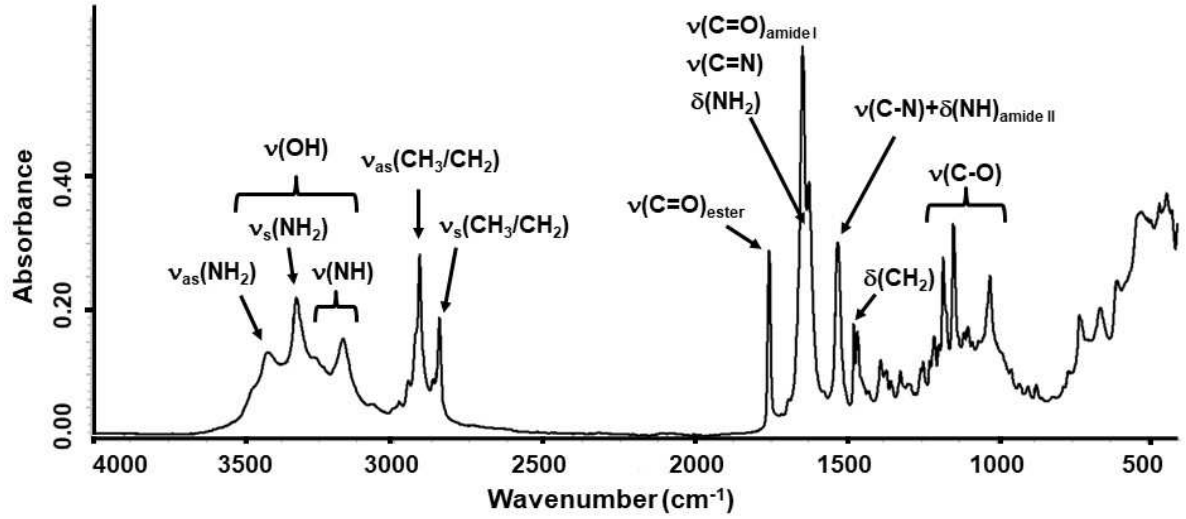

Fig. 4. ATR/FT-IR spectra of LAE formulation (Mirenat-D).

3.4. Thickness

The thickness value is a crucial parameter for determining final physical, mechanical and barrier properties of biodegradable films. The thickness values of control and active films are reported in Tab. 1. Thickness values ranged from 44.81 to 59.82 µm. The control film showed the lowest value ($p<0.05$). This is due to the well-organized and dense network structure in the CS-PVA blend film as confirmed by SEM images. The incorporation of LAE into the CS-PVA blend increased the thickness ($p<0.05$) and the CS-PVA film enriched with 10% LAE showed the highest thickness value ($p<0.05$). In this study, all films were prepared by casting a constant amount of FFS in Petri dishes with the same surface ratio, therefore differences in thickness between control and active films are due to the addition of LAE to the FFS. According to Gaikwad et al. (2017), film thickness is influenced by the solid content of the FFS. Thus, LAE might contribute to loosen film matrix, reduce the homogeneity, and consequently increase the thickness. In contrast, Rubilar et al., (2016) reported that addition of LAE to CS films did not influence the thickness. It is noteworthy that the type of LAE applied in different studies as a powder (Mirenat-D or Mirenat-P) or dissolved in glycerol (Mirenat-G) strongly affects film thickness.

3.5. Mechanical properties

The tensile strength (TS), elongation at break (E%) and elastic modulus (EM) are three important parameters for evaluation of mechanical properties. Generally, adequate mechanical strength and extensibility are required for the development of biodegradable films for food packaging applications. The mechanical properties of control and active films are presented in Tab. 1. The control film showed the highest TS, E% and EM values. The presence of LAE greatly influenced TS and E% ($p<0.05$). Films containing LAE were less resistant and less stretchable than the control film ($p<0.05$). Incorporation of LAE up to 10% decreased the tensile strength from 42.48 to 15.70 MPa and E% from 54.25 to 14.31%. The significant deterioration of mechanical properties above 2.5% incorporation of LAE (Tab. 1) is also consistent with the ATR/FT-IR observation, that band shifts and intensity changes occur above this threshold concentration. This tendency could be explained by the fact that active films containing a high concentration of LAE are unable to form a cohesive and continuous matrix as it was confirmed by SEM analysis. This can be attributed to the competitive interaction of the functional groups of LAE and the CS-PVA blend that limit cohesion forces within the polymer in the film matrix and consequently decrease the degree of physical crosslinking by weakening the intermolecular hydrogen bonding, thereby resulting in the reduction of mechanical properties. Despite the reduction of TS after incorporation of LAE, it should be noted that the TS values for the active films containing LAE up to 2.5% were comparable with those of plastic films that are used widely in the market, such as high density polyethylene (22-31 MPa) and polypropylene (31-38 MPa) but slightly lower than that for polystyrene (45-83 MPa) (Theinsathid, Visessanguan, Kruenate, Kingcha, & Keeratipibul, 2012). Moreno, Díaz, Atarés, & Chiralt (2016) also reported that the incorporation of LAE into starch-gelatin blend film notably reduced the stiffness and resistance to break compared to the control film. In contrast to these results, Rubilar et al. (2016) reported that the incorporation of LAE (1g/L) to CS films significantly increased TS and E% values ($p<0.05$) which might be due to the application of Mirenat-G (10% LAE, 90% glycerol) as LAE source. Hence the observed effect could be mainly due to the plasticizing effect of glycerol. Literature data regarding mechanical properties are controversial and are influenced by multiple factors

such as the molecular mass of the polymer, deacetylation degree of CS, degree of hydrolysis of PVA, pH of the FFS, drying conditions and type of LAE.

Table 1
Thickness, tensile strength (TS), elongation at break (E%) and elastic modulus (EM) of the films based on control CS-PVA blend (CS-PVA) and CS-PVA enriched with LAE (1-10% w/w).

Film sample	Thickness (μm)	TS (MPa)	E (%)	EM (MPa)
CS-PVA	44.8 ± 1.0^{a}	42.5 ± 1.6^{d}	54.2 ± 2.0^{d}	1570.1 ± 139.0^{d}
CS-PVA-LAE 1%	45.1 ± 0.5^{a}	33.0 ± 2.4^{c}	38.9 ± 3.1^{c}	1153.1 ± 121.1^{bc}
CS-PVA-LAE 2.5%	49.9 ± 1.6^{b}	34.5 ± 4.2^{c}	39.0 ± 2.6^{c}	1287.3 ± 77.8^{c}
CS-PVA-LAE 5%	54.9 ± 2.7^{c}	22.2 ± 0.9^{b}	25.0 ± 2.8^{b}	1016.9 ± 90.8^{b}
CS-PVA-LAE 10%	59.6 ± 0.8^{d}	15.7 ± 1.2^{a}	14.3 ± 1.9^{a}	701.3 ± 53.8^{a}

Values are given as mean ± SD (n = 3).
Different letters in the same column indicate significant differences ($p<0.05$).

3.6. UV barrier, light transmittance and opacity value

Protecting food from the effect of UV-Vis radiation is one of the desired characteristics of packaging material due to their influence on product performance and consumer acceptance. The UV-Vis light transmittance of control and active films in the wavelength range of 200–800 nm is presented in Fig. 5. Control film showed a higher UV light transmittance (200–350 nm) compared to the active films. UV light transmittance was reduced at increasing LAE concentration and active films behaved as effective UV barriers at 200 nm since the transmittance value was below 1%. UV barrier property of films is an important parameter for food packaging applications to minimize UV-induced lipid oxidation, to preserve the organoleptic properties of the packaged food, to avoid nutrient losses, discoloration and off-flavors, thereby prolonging food shelf life (Hajji et al., 2016; Wu, Sun, Guo, Ge, & Zhang, 2017).

The transmission of visible light (400–800 nm) was higher than 80% for the control film. The active films containing 1 and 2.5% LAE showed similar results while active films containing 5 and 10% LAE showed lower values. Thus, once a critical LAE concentration is exceeded, aggregates are formed, that were large enough to scatter the light and thereby interfere with

its transmission (Bonnaud, Weiss, & McClements, 2010). The light barrier property is also an important factor for food preservation to avoid photo-oxidation of organic compounds and degradation of vitamins and other pigments. In addition, it provides a clear view of the food content and its condition (Figueroa-Lopez, Andrade-Mahecha, & Torres-Vargas, 2018; Yadav & Chiu, 2019). In this study, all films can be considered as transparent due to the opacity value lower than 5 at 600 nm (Tab. 2). The higher value of this parameter represents the lower transparency of the film.

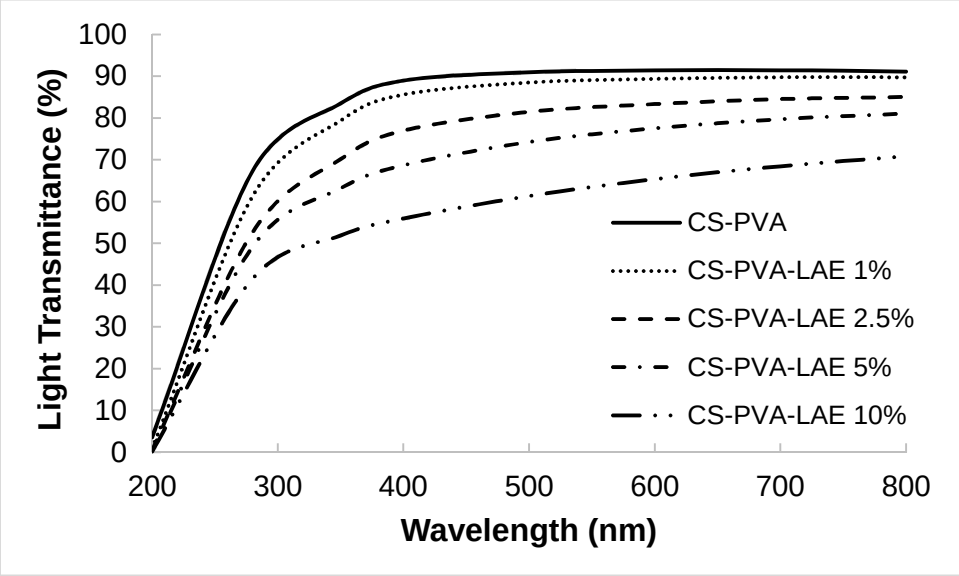

Fig. 5. UV-Vis light transmittance of the films based on a control CS-PVA blend (CS-PVA) and CS-PVA blends enriched with LAE (1-10% w/w).

3.7. Color

The color values (L*, a* and b*) and total color difference (ΔE*) of control and active films are shown in Tab. 2. The L*, a*, b* offer objective evaluation of the appearance of films while ΔE* measures the color change of treatment from a reference color. Color is an important feature of a film for food packaging applications since it evaluates the visual characteristic of the food product inside the packaging system and affects consumer purchase decision. The L* value indicates lightness and represents the apparent proportion of incident light reflected by an object, varying between 98.22 and 98.99, which means that all the films were almost clear. No significant differences ($p>0.05$) for L* between the control and active films were found. These results were in agreement with opacity values that showed all films were clear and transparent. The a* value, expressing the green-red color component, was negative for

all films, which means that films were not truly red (Virginia Muriel-Galet, López-Carballo, Hernández-Muñoz, & Gavara, 2014). The b* value measures the blue-yellow color component. This value increased upon addition of LAE ($p<0.05$), suggesting a gain of slight yellow color. ΔE* was used to compare the color of active films with commercial plastic films (perceptibility threshold of ΔE* = 1). The selected value is often used as the smallest color difference that the human eye can detect (Thakhiew, Devahastin, & Soponronnarit, 2013). Control film had ΔE* value of 0.91. The ΔE* increased upon addition of LAE ($p<0.05$) and reached a value of 1.70 in the active film containing 10% LAE. This behavior might be attributed to the increase in the colorimetric coordinate b* and increase in film thickness upon addition of LAE. In summary, the consumer might not be able to detect color difference in active films, despite the slightly higher values than the threshold. A similar result has been reported by Rubilar et al. (2016).

Table 2
Color parameters (L*, a* and b*), total color difference (ΔE*) and opacity values of the films based on a control CS-PVA blend (CS-PVA) and CS-PVA enriched with LAE (1-10% w/w).

Film sample	Color parameters				Opacity value
	L*	a*	b*	ΔE*	(600 nm)
CS-PVA	99.0 ± 0.2^{a}	-0.3 ± 0.03^{c}	0.7 ± 0.1^{a}	0.91 ± 0.2^{a}	0.9 ± 0.01^{a}
CS-PVA-LAE 1%	98.8 ± 0.1^{a}	-0.3 ± 0.01^{c}	0.7 ± 0.1^{a}	0.99 ± 0.1^{a}	1.1 ± 0.08^{ab}
CS-PVA-LAE 2.5%	98.8 ± 0.1^{a}	-0.4 ± 0.02^{b}	1.0 ± 0.1^{b}	1.22 ± 0.1^{b}	1.6 ± 0.31^{bc}
CS-PVA-LAE 5%	98.6 ± 0.1^{a}	-0.4 ± 0.03^{a}	1.3 ± 0.2^{c}	1.63 ± 0.2^{c}	2.0 ± 0.13^{c}
CS-PVA-LAE 10%	98.7 ± 0.2^{a}	-0.5 ± 0.02^{a}	1.4 ± 0.1^{c}	1.70 ± 0.1^{c}	3.1 ± 0.27^{d}

Values are given as mean ± SD (n = 3).
Different letters in the same column indicate significant differences ($p<0.05$).

3.8. Moisture content, water solubility, water vapor transmission rate and water vapor permeability

One of the major drawbacks of biodegradable films for food packaging applications is their sensitivity to water. Due to the hydrophilic nature of CS and PVA, when these films are exposed to high relative humidity conditions, water molecules are absorbed by the polymeric chains, exerting a plasticizing effect and resulting in changes of the mechanical and barrier

properties (Aguirre-Loredo, Rodríguez-Hernández, Morales-Sánchez, Gómez-Aldapa, & Velazquez, 2016). Therefore, measuring water sensitivity plays an important role in the packaging performance for the food products. The moisture content (MC), water solubility (WS), water vapor transmission rate (WVTR) and water vapor permeability (WVP) of control and active films are presented in Tab. 3.

The MC value ranged from 16.42 to 17.53%. The effect of LAE incorporation on the MC was not significant ($p<0.05$). Moreno, Gil, Atarés, & Chiralt (2017b) reported that the enrichment of starch-gelatin films with different LAE concentrations did not influence the MC. Solubility is defined as the content of dry matter solubilized after 24 h immersion in water. The control film showed the lowest WS value and addition of LAE increased the WS value. CS-PVA film containing 10% LAE showed the highest WS value ($p<0.05$). The higher solubility values of active films could be explained by the hydrophilic nature of CS-PVA blend film and low oil-water equilibrium partition coefficient of LAE ($K_{ow}<0.1$), which means that LAE has a high affinity to water molecules (Higueras et al., 2013; Rubilar et al., 2016).

The barrier properties of biodegradable films to water play an important role in determining the shelf life of packed foodstuffs (Del Nobile, Fava, & Piergiovanni, 2002). In this study, the WVTR was not significantly influenced by the addition of LAE, despite showing higher values in active films ($p>0.05$). However, the incorporation of LAE to CS-PVA blend film increased the WVP value. This might be due to the difference in each film thickness considered in WVP calculation (Rubilar et al., 2016). Additionally, incorporation of LAE into the CS-PVA film network may break hydrogen bonding and disrupt the long-range ordering between CS and PVA molecules, resulting in an increase in WVP value (Ma, Zhang, & Zhong, 2016).

Table 3

Moisture content (MC), water solubility (WS), water vapor transmission rate (WVTR) and water vapor permeability (WVP) of the films based on a control CS-PVA blend (CS-PVA) and CS-PVA enriched with LAE (1-10% w/w).

Film sample	MC (%)	WS (%)	WVTR (g /day m^2)	WVP 90:0% RH (g mm/kP day m^2)
CS-PVA	16.4 ± 0.5^{a}	22.1 ± 0.4^{a}	3605.6 ± 450.8^{a}	18 ± 0.02^{a}
CS-PVA-LAE 1%	16.7 ± 0.9^{a}	23.7 ± 2.8^{ab}	3608.7 ± 362.1^{a}	19 ± 0.02^{a}

CS-PVA-LAE 2.5%	16.8 ± 0.7^{a}	25.4 ± 3.4^{ab}	3729.5 ± 369.3^{a}	21 ± 0.02^{ab}
CS-PVA-LAE 5%	17.1 ± 0.6^{a}	27.8 ± 2.1^{b}	3742.1 ± 341.5^{a}	24 ± 0.02^{b}
CS-PVA-LAE 10%	17.5 ± 0.6^{a}	33.2 ± 2.1^{c}	3808.9 ± 337.7^{a}	26 ± 0.02^{c}

Values are given as mean ± SD (n = 3).
Different letters in the same column indicate significant differences ($p<0.05$).

3.9. In vitro antimicrobial activity

3.9.1. Disk diffusion assay

The antimicrobial activity of control and active films against common bacterial food pathogens, namely *C. jejuni*, *E. coli*, *L. monocytogenes* and *S. typhimurium*, was evaluated by the disk diffusion assay (Fig. 6) and the details are presented in Tab. 4. The control film did not show an inhibition zone against any of the tested microorganisms. The absence of inhibition zone could be explained by the limitation of CS to diffuse in agar medium (Leceta, Guerrero, Ibarburu, Dueñas, & De La Caba, 2013) and incapability of PVA to inhibit bacterial growth as it has been reported by other authors (Hajji et al., 2016; Tripathi et al., 2009), so that only microorganisms in direct contact with the active sites of CS in the CS-PVA film network are inhibited. Active films containing 1% LAE were only effective against *C. jejuni*. In general, LAE was more effective against *C. jejuni* compared to the other microorganisms considered, which showed inhibition haloes ranging from 3 to 5-fold wider. No differences were observed in the inhibition zones produced by CS-PVA films incorporating 5 and 10% of LAE against all tested microorganisms. Similar results reported by Muriel-Galet, López-Carballo, Gavara, & Hernández-Muñoz (2015). Pattanayaiying, H-Kittikun, & Cutter (2015) also found that incorporation of LAE into pullulan film inhibited the growth of foodborne pathogens such as *Salmonella spp*., *L. monocytogenes* and *E. coli.* The antimicrobial activity of LAE is attributed to its action as a cationic surfactant on the cytoplasmic membranes of microorganisms, causing a disturbance in membrane potential and resulting in cell growth inhibition and loss of viability (Kashiri et al., 2016; Muriel-Galet, López-Carballo, Gavara, & Hernández-Muñoz, 2012).

Table 4
Inhibition zone diameters of the film disks (22 mm diameter) based on a control CS-PVA blend (CS-PVA) and CS-PVA enriched with LAE (1-10% w/w).

Film sample	*L. monocytogenes*	*E. coli*	*C. jejuni*	*S. typhimurium*
CS-PVA	N. D.	N. D.	N. D.	N. D.
CS-PVA-LAE 1%	N. D.	N. D.	1.8 ± 1.0^{aA}	N. D.
CS-PVA-LAE 2.5%	0.5 ± 0.5^{aA}	0.6 ± 0.3^{aA}	3.7 ± 1.5^{bB}	0.6 ± 0.7^{aA}
CS-PVA-LAE 5%	1.3 ± 0.7^{abA}	1.2 ± 0.9^{abA}	4.6 ± 1.8^{bB}	1.7 ± 1.1^{abA}
CS-PVA-LAE 10%	1.6 ± 0.9^{bA}	1.6 ± 1.0^{bA}	5.2 ± 1.4^{bB}	1.8 ± 1.8^{aA}

Values are given as mean ± SD (n = 3). N.D: not detected.
Different lowercase letters in the same column indicate significant differences ($p<0.05$).
Different capital letters in the same row indicate significant differences ($p<0.05$).

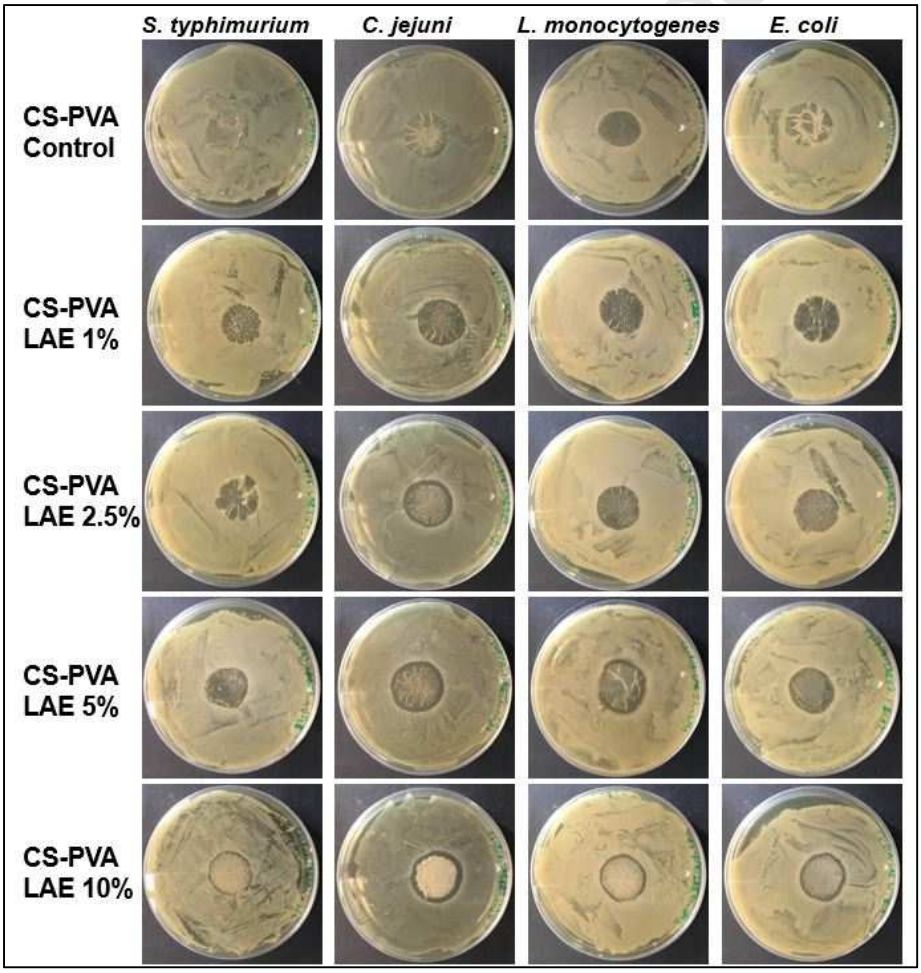

Fig. 6. Disk diffusion results of films based on a control CS-PVA blend (CS-PVA) and CS-PVA enriched with LAE (1-10% w/w).

3.9.2. Evaluation of antimicrobial activity in liquid medium

The Antimicrobial activity of control and active films against common bacterial food pathogens including *C. jejuni*, *E. coli*, *L. monocytogenes* and *S. typhimurium* was also evaluated in liquid medium and the details are presented in Tab. 5. CS-PVA film without LAE

used as a control. Among tested microorganisms *C. jejuni* showed higher log reduction (2) for CS-PVA-LAE 10% films that is in agreement with the DDA result. The incorporation of LAE (1-10%) showed a log reduction against all tested microorganisms. Clearly, the higher the LAE concentration in the film, the greater the antimicrobial efficiency of the CS-PVA film. Similar result were reported by (V. Muriel-Galet et al., 2015) and (Kashiri et al., 2016).

Table 5
Antimicrobial activity of films based on a control CS-PVA blend (CS-PVA) and CS-PVA enriched with LAE (1- 10% w/w) expressed as logarithm of colony forming units (log CFU/ mL) and log reduction value (LRV).

Film sample	***L. monocytogenes***		***E. coli***		***C. jejuni***		***S. typhimurium***	
	log (cfu/mL)	*LRV*	*log (cfu/mL)*	*LRV*	*log (cfu/mL)*	*LRV*	*log (cfu/mL)*	*LRV*
CS-PVA	9.2 ± 0.2^{b}		9.3 ± 0.1^{c}		9.4 ± 0.1^{b}		9.5 ± 0.1^{c}	
CS-PVA-LAE1%	9.2 ± 0.2^{b}	0	9.1 ± 0.1^{bc}	0.2	9.2 ± 0.1^{b}	0.2	9.4 ± 0.1^{bc}	0.1
CS-PVA-LAE2.5%	9.0 ± 0.2^{b}	0.2	9.0 ± 0.1^{bc}	0.3	9.1 ± 0.3^{b}	0.3	9.3 ± 0.1^{bc}	0.2
CS-PVA-LAE5%	8.9 ± 0.2^{b}	0.3	8.8 ± 0.1^{b}	0.5	8.8 ± 0.1^{b}	0.6	9.2 ± 0.1^{ab}	0.3
CS-PVA-LAE10%	7.7 ± 0.8^{a}	1.5	8.3 ± 0.4^{a}	1	7.4 ± 0.1^{a}	2	9.1 ± 0.1^{a}	0.4

Values are given as mean ± SD (n = 3).
Different lowercase letters in the same column indicate significant differences ($p<0.05$).

4. Conclusion

In this study, biodegradable active films based on CS-PVA blends enriched with LAE at different concentrations (1-10%, w/w) were developed and their microstructural, physical, optical, mechanical, barrier and antimicrobial properties were evaluated for food packaging applications. The results showed that all films containing LAE were transparent. The incorporation of LAE could improve the UV and light barrier properties of CS-PVA film, which may be useful to protect food from UV degradation and photo-oxidation. The characteristic absorption bands in the ATR/FT-IR spectra of the CS-PVA blends did not show significant band shifts and intensity changes up to 2.5% LAE content, indicating low interactions between the polymer and the LAE. However, at elevated LAE content the C=O, NH_2 and NH functionalities of this additive contribute to competitive molecular interactions with the

hydroxyl, amino, ether and residual acetate groups of the CS-PVA film network. The presence of LAE greatly influenced TS and E%. Films with LAE were less resistant and less stretchable than the control film and a significant deterioration of mechanical properties occurred above 2.5% incorporation of LAE. The developed active films, especially those including 5 and 10% LAE, were effective against common bacterial food pathogens. The results suggest that the CS-PVA films enriched with different concentrations of LAE could be considered as environmentally friendly packaging material with antimicrobial properties to extend the shelf life of food products and that might be an alternative to synthetic plastics for certain applications.

Declaration of interest

None.

Acknowledgements

The authors would like to thank Dr. Massimo Tonelli and Centro Interdipartimentale Grandi Strumenti (CIGS) of the University of Modena and Reggio Emilia for assistance in the SEM and AFM measurements.

References

1. Aguirre-Loredo, R. Y., Rodríguez-Hernández, A. I., Morales-Sánchez, E., Gómez-Aldapa, C. A., & Velazquez, G. (2016). Effect of equilibrium moisture content on barrier, mechanical and thermal properties of chitosan films. *Food Chemistry*, *196*, 560–566. https://doi.org/10.1016/j.foodchem.2015.09.065
2. Aloui, H., Khwaldia, K., Hamdi, M., Fortunati, E., Kenny, J. M., Buonocore, G. G., & Lavorgna, M. (2016). Synergistic effect of halloysite and cellulose nanocrystals on the functional properties of PVA based nanocomposites. *ACS Sustainable Chemistry and Engineering*, *4*(3), 794–800. https://doi.org/10.1021/acssuschemeng.5b00806
3. ASTM. (2001a). Standard test method for tensile properties of thin plastic sheeting. In *Annual books of ASTM standards. Designation D882-01. Philadelphia: ASTM, American Society for Testing Materials.*
4. ASTM. (2001b). Standard test method for water vapor transmission of materials. In

Annual books of ASTM Standards. Designation E 96-01, Philadelphia: ASTM, American Society for Testing Materials

5. Becerril, R., Manso, S., Nerin, C., & Gómez-Lus, R. (2013). Antimicrobial activity of Lauroyl Arginate Ethyl (LAE), against selected food-borne bacteria. *Food Control*, *32*(2), 404–408. https://doi.org/10.1016/j.foodcont.2013.01.003
6. Bellelli, M., Licciardello, F., Pulvirenti, A., & Fava, P. (2018). Properties of poly(vinyl alcohol) films as determined by thermal curing and addition of polyfunctional organic acids. *Food Packaging and Shelf Life*, *18*, 95–100. https://doi.org/10.1016/j.fpsl.2018.10.004
7. Bonilla, J., Fortunati, E., Atarés, L., Chiralt, A., & Kenny, J. M. (2014). Physical, structural and antimicrobial properties of poly vinyl alcohol- chitosan biodegradable films. *Food Hydrocolloids*, *35*, 463–470. https://doi.org/10.1016/j.foodhyd.2013.07.002
8. Bonnaud, M., Weiss, J., & McClements, D. J. (2010). Interaction of a food-grade cationic surfactant (Lauric Arginate) with food-grade biopolymers (pectin, carrageenan, xanthan, alginate, dextran, and chitosan). *Journal of Agricultural and Food Chemistry*, *58*(17), 9770–9777. https://doi.org/10.1021/jf101309h
9. Cazón, P., Vázquez, M., & Velazquez, G. (2018). Composite films of regenerate cellulose with chitosan and polyvinyl alcohol: Evaluation of water adsorption, mechanical and optical properties. *International Journal of Biological Macromolecules*, *117*, 235–246. https://doi.org/10.1016/j.ijbiomac.2018.05.148
10. Costa-junior, E. D. S., Pereira, M. M., & Mansur, H. S. (2009). Properties and biocompatibility of chitosan films modified by blending with PVA and chemically crosslinked. *Journal of Materials Science: Materials in Medicine, 20*(2), 553–561. https://doi.org/10.1007/s10856-008-3627-7
11. De Leo, R., Quartieri, A., Haghighi, H., Gigliano, S., Bedin, E., & Pulvirenti, A. (2018). Application of pectin-alginate and pectin-alginate-lauroyl arginate ethyl coatings to eliminate Salmonella enteritidis cross contamination in egg shells. *Journal of Food*

Safety, *38*(6) 1-9. https://doi.org/10.1111/jfs.12567

12. Del Nobile, M. A., Fava, P., & Piergiovanni, L. (2002). Water transport properties of cellophane flexible films intended for food packaging applications. *Journal of Food Engineering*, *53*(4), 295–300. https://doi.org/10.1016/S0260-8774(01)00168-6
13. EFSA. (2007). Opinion of the Scientific Panel on Food Additives, Flavourings, Processing Aids and Materials in Contact with Food on a request from the Commission related to an application on the use of ethyl lauroyl arginate as a food additive, LAMIRSA, 2008. *The EFSA Journal*, *511*, 1–27.
14. Figueroa-Lopez, K. J., Andrade-Mahecha, M. M., & Torres-Vargas, O. L. (2018). Development of antimicrobial biocomposite films to preserve the quality of bread. *Molecules*, *23*(1), 212. https://doi.org/10.3390/molecules23010212
15. Gaikwad, K. K., Lee, S. M., Lee, J. S., & Lee, Y. S. (2017). Development of antimicrobial polyolefin films containing lauroyl arginate and their use in the packaging of strawberries. *Journal of Food Measurement and Characterization*, *11*(4), 1706–1716. https://doi.org/10.1007/s11694-017-9551-0
16. Gamarra, A., Missagia, B., Urpí, L., Morató, J., & Muñoz-guerra, S. (2018). Ionic coupling of hyaluronic acid with ethyl *N*-lauroyl $_{L}$-arginate (LAE): Structure, properties and biocide activity of complexes. *Carbohydrate Polymers*, *197*, 109–116. https://doi.org/10.1016/j.carbpol.2018.05.057
17. Ghaderi, J., Hosseini, S. F., Keyvani, N., Gómez-Guillén, M. C. (2019). Polymer blending effects on the physicochemical and structural features of the chitosan/poly(vinyl alcohol)/fish gelatin ternary biodegradable films. *Food Hydrocolloids,* 95, 122–132 https://doi.org/10.1016/j.foodhyd.2019.04.021
18. Gontard, N., Guilbert, S., & Cuq, J. (1992). Edible Wheat Gluten Films: Influence of the Main Process Variables on Film Properties using Response Surface Methodology. Journal of Food Science, 57(1), 190–195. https://doi.org/10.1111/j.1365-2621.1992.tb05453.x
19. Haghighi, H., De Leo, R., Bedin, E., Pfeifer, F., Siesler, H. W., & Pulvirenti, A.

(2019a). Comparative analysis of blend and bilayer films based on chitosan and gelatin enriched with LAE (lauroyl arginate ethyl) with antimicrobial activity for food packaging applications. *Food Packaging and Shelf Life*, *19*, 31–39. https://doi.org/10.1016/j.fpsl.2018.11.015

20. Haghighi, H., Biard, S., Bigi, F., Leo, R. De, Bedin, E., Pfeifer, F., Siesler, HW., Licciardello, F., Pulvirenti, A. (2019b). Comprehensive characterization of active chitosan-gelatin blend films enriched with different essential oils. *Food Hydrocolloids*, *95*, 33–42. https://doi.org/10.1016/j.foodhyd.2019.04.019
21. Hajji, S., Chaker, A., Jridi, M., Maalej, H., Jellouli, K., Boufi, S., & Nasri, M. (2016). Structural analysis, and antioxidant and antibacterial properties of chitosan-poly (vinyl alcohol) biodegradable films. *Environmental Science and Pollution Research*, *23* (15), 15310–15320. https://doi.org/10.1007/s11356-016-6699-9
22. Higueras, L., López-Carballo, G., Hernández-Muñoz, P., Gavara, R., & Rollini, M. (2013). Development of a novel antimicrobial film based on chitosan with LAE (ethyl-N^{α}-dodecanoyl-L-arginate) and its application to fresh chicken. *International Journal of Food Microbiology*, *165*(3), 339–345. https://doi.org/10.1016/j.ijfoodmicro.2013.06.003
23. Jahan, F., Mathad, R. D., & Farheen, S. (2016). Effect of mechanical strength on chitosan-pva blend through ionic crosslinking for food packaging application. *Materials Today: Proceedings-Part B*, *3*(10), 3689–3696. https://doi.org/10.1016/j.matpr.2016.11.014
24. Kanatt, S. R., Rao, M. S., Chawla, S. P., & Sharma, A. (2012). Active chitosan-polyvinyl alcohol films with natural extracts. *Food Hydrocolloids*, *29*(2), 290–297. https://doi.org/10.1016/j.foodhyd.2012.03.005
25. Kashiri, M., Cerisuelo, J. P., Domínguez, I., López-Carballo, G., Hernández-Muñoz, P., & Gavara, R. (2016). Novel antimicrobial zein film for controlled release of lauroyl arginate (LAE). *Food Hydrocolloids*, *61*, 547–554. https://doi.org/10.1016/j.foodhyd.2016.06.012

26. Kim, J. H., Kim, J. Y., Lee, Y. M., & Kim, K. Y. (1992). Properties and swelling characteristics of cross-linked poly (vinyl alcohol)/ chitosan blend membrane. *Journal of Applied Polymer Science*, *45*(10), 1711–1717. https://doi.org/10.1002/app.1992.070451004
27. Koosha, M., & Mirzadeh, H. (2015). Electrospinning, mechanical properties, and cell behavior study of chitosan/PVA nanofibers. *Journal of Biomedical Materials Research - Part A*, *103*(9), 3081–3093. https://doi.org/10.1002/jbm.a.35443
28. Kumar, S., Krishnakumar, B., Sobral, A. J. F. N., & Koh, J. (2019). Bio-based (chitosan/PVA/ ZnO) nanocomposites film : Thermally stable and photoluminescence material for removal of organic dye. *Carbohydrate Polymers*, *205*, 559–564. https://doi.org/10.1016/j.carbpol.2018.10.108
29. Leceta, I., Guerrero, P., & De La Caba, K. (2013). Functional properties of chitosan-based films. *Carbohydrate Polymers*, *93*(1), 339–346. https://doi.org/10.1016/j.carbpol.2012.04.031
30. Leceta, I., Guerrero, P., Ibarburu, I., Dueñas, M. T., & De La Caba, K. (2013). Characterization and antimicrobial analysis of chitosan-based films. *Journal of Food Engineering*, *116*(4), 889–899. https://doi.org/10.1016/j.jfoodeng.2013.01.022
31. Liu, Y., Wang, S., & Lan, W. (2018). Fabrication of antibacterial chitosan-PVA blended film using electrospray technique for food packaging applications. *International Journal of Biological Macromolecules-Part A*, *107*, 848–854. https://doi.org/10.1016/j.ijbiomac.2017.09.044
32. Ma, Q., Zhang, Y., & Zhong, Q. (2016). Physical and antimicrobial properties of chitosan films incorporated with lauric arginate, cinnamon oil, and ethylenediaminetetraacetate. *LWT - Food Science and Technology*, *65*, 173–179. https://doi.org/10.1016/j.lwt.2015.08.012
33. Moreno, O., Cárdenas, J., Atarés, L., & Chiralt, A. (2017a). Influence of starch oxidation on the functionality of starch-gelatin based active films. *Carbohydrate Polymers*, *178*, 147–158. https://doi.org/10.1016/j.carbpol.2017.08.128

683 34. Moreno, O., Díaz, R., Atarés, L., & Chiralt, A. (2016). Influence of the processing
684 method and antimicrobial agents on properties of starch-gelatin biodegradable films.
685 *Polymer International*, *65*(8), 905–914. https://doi.org/10.1002/pi.5115
686 35. Moreno, O., Gil, À., Atarés, L., & Chiralt, A. (2017b). Active starch-gelatin films for
687 shelf-life extension of marinated salmon. *LWT - Food Science and Technology*, *84*,
688 189–195. https://doi.org/10.1016/j.lwt.2017.05.005
689 36. Muriel-Galet, V., Carballo, G. L., Hernández-Muñoz, P., & Gavara, R. (2016). Ethyl
690 Lauroyl Arginate (LAE): usage and potential in antimicrobial packaging. In J. Barros-
691 Velazquez (Ed), *Antimicrobial Food Packaging* (pp. 313–318). Academic Press.
692 https://doi.org/10.1016/B978-0-12-800723-5.00024-3
693 37. Muriel-Galet, López-Carballo, G., Gavara, R., & Hernández-Muñoz, P. (2015).
694 Antimicrobial effectiveness of lauroyl arginate incorporated into ethylene vinyl alcohol
695 copolymers to extend the shelf-life of chicken stock and surimi sticks. *Food and*
696 *Bioprocess Technology*, *8*(1), 208–217. https://doi.org/10.1007/s11947-014-1391-x
697 38. Muriel-Galet, V., López-Carballo, G., Hernández-Muñoz, P., & Gavara, R. (2014).
698 Characterization of ethylene-vinyl alcohol copolymer containing lauril arginate (LAE)
699 as material for active antimicrobial food packaging. *Food Packaging and Shelf Life*,
700 *1*(1), 10–18. https://doi.org/10.1016/j.fpsl.2013.09.002
701 39. Muriel-Galet, V., López-Carballo, G., Gavara, R., & Hernández-Muñoz, P. (2012).
702 Antimicrobial food packaging film based on the release of LAE from EVOH.
703 *International Journal of Food Microbiology*, *157*(2), 239–244.
704 https://doi.org/10.1016/j.ijfoodmicro.2012.05.009
705 40. Parida, U. K., Nayak, A. K., Binhani, B. K., & Nayak, P. L. (2011). Synthesis and
706 characterization of chitosan-polyvinyl alcohol blended with cloisite 30B for controlled
707 release of the anticancer drug curcumin. *Journal of Biomaterials and*
708 *Nanobiotechnology*, *2*, 414–425. https://doi.org/10.4236/jbnb.2011.24051
709 41. Pattanayaiying, R., H-Kittikun, A., & Cutter, C. N. (2015). Incorporation of nisin Z and
710 lauric arginate into pullulan films to inhibit foodborne pathogens associated with fresh

and ready-to-eat muscle foods. *International Journal of Food Microbiology*, *207*, 77–82. https://doi.org/10.1016/j.ijfoodmicro.2015.04.045

42. Pavaloiu, R. D., Stoica-Guzun, A., Stroescu, M., Jinga, S. I., & Dobre, T. (2014). Composite films of poly(vinyl alcohol)-chitosan-bacterial cellulose for drug controlled release. *International Journal of Biological Macromolecules*, *68*, 117–124. https://doi.org/10.1016/j.ijbiomac.2014.04.040
43. Pereira Jr, V. A., de Arruda, I. N. Q., & Stefani, R. (2015). Active chitosan/PVA films with anthocyanins from *Brassica oleraceae* (Red Cabbage) as Time-Temperature Indicators for application in intelligent food packaging. *Food Hydrocolloids*, *43*, 180–188. https://doi.org/10.1016/j.foodhyd.2014.05.014
44. Rubilar, J. F., Candia, D., Cobos, A., Díaz, O., & Pedreschi, F. (2016). Effect of nanoclay and ethyl-N^{α}-dodecanoyl-*L*-arginate hydrochloride (LAE) on physicomechanical properties of chitosan films. *LWT - Food Science and Technology*, *72*, 206–214. https://doi.org/10.1016/j.lwt.2016.04.057
45. Sarwar, M. S., Niazi, M. B. K., Jahan, Z., Ahmad, T., & Hussain, A. (2018). Preparation and characterization of PVA/nanocellulose/Ag nanocomposite films for antimicrobial food packaging. *Carbohydrate Polymers*, *184*, 453–464. https://doi.org/10.1016/j.carbpol.2017.12.068
46. Thakhiew, W., Devahastin, S., & Soponronnarit, S. (2013). Physical and mechanical properties of chitosan films as affected by drying methods and addition of antimicrobial agent. *Journal of Food Engineering*, *119*(1), 140–149. https://doi.org/10.1016/j.jfoodeng.2013.05.020
47. Theinsathid, P., Visessanguan, W., Kruenate, J., Kingcha, Y., & Keeratipibul, S. (2012). Antimicrobial activity of lauric arginate-coated polylactic acid films against *Listeria monocytogenes* and *Salmonella* Typhimurium on cooked sliced ham. *Journal of Food Science*, *77*(2), 142–149. https://doi.org/10.1111/j.1750-3841.2011.02526.x
48. Tripathi, S., Mehrotra, G. K., & Dutta, P. K. (2009). Physicochemical and bioactivity of cross-linked chitosan–PVA film for food packaging applications. *International Journal*

739 *of Biological Macromolecules*, *45(4)*, 372–376.
740 https://doi.org/10.1016/j.ijbiomac.2009.07.006
741 49. Tripathi, S., Mehrotra, G. K., & Dutta, P. K. (2008). Chitosan based antimicrobial films
742 for food packaging applications. *e-Polymers*. *8*(1), 093.
743 https://doi.org/10.1515/epoly.2008.8.1.1082
744 50. USFDA. (2005). Center for Food Safety and Applied Nutrition, U.S. *Agency Response*
745 *Letter GRAS Notice No. GRN 000164.*
746 51. Wu, J., Sun, X., Guo, X., Ge, S., & Zhang, Q. (2017). Physicochemical properties,
747 antimicrobial activity and oil release of fish gelatin films incorporated with cinnamon
748 essential oil. *Aquaculture and Fisheries*, *2*(4), 185–192.
749 https://doi.org/10.1016/j.aaf.2017.06.004
750 52. Yadav, M., & Chiu, F. C. (2019). Cellulose nanocrystals reinforced κ-carrageenan
751 based UV resistant transparent bionanocomposite films for sustainable packaging
752 applications. *Carbohydrate Polymers*, *211*, 181–194.
753 https://doi.org/10.1016/j.carbpol.2019.01.114

Highlights:

- LAE was effectively incorporated into chitosan-polyvinyl alcohol films
- High LAE levels negatively affected mechanical and water barrier properties
- Addition of LAE improved UV barrier of chitosan-polyvinyl alcohol blend films
- The developed active films were effective against four food bacterial pathogens

Conflicts of Interest Statement

Manuscript title: Development of antimicrobial films based on chitosan-polyvinyl alcohol blend enriched with ethyl lauroyl arginate (LAE) for food packaging applications

The authors whose names are listed immediately below certify that they have NO affiliations with or involvement in any organization or entity with any financial interest (such as honoraria; educational grants; participation in speakers' bureaus; membership, employment, consultancies, stock ownership, or other equity interest; and expert testimony or patent-licensing arrangements), or non-financial interest (such as personal or professional relationships, affiliations, knowledge or beliefs) in the subject matter or materials discussed in this manuscript.

Author names:

1- Hossein Haghighi
2- Serge Kameni Leugoue
3- Frank Pfeifer
4- Heinz Wilhelm Siesler
5- Fabio Licciardello
6- Patrizia Fava
7- Andrea Pulvirenti

The authors whose names are listed immediately below report the following details of affiliation or involvement in an organization or entity with a financial or non-financial interest in the subject matter or materials discussed in this manuscript. Please specify the nature of the conflict on a separate sheet of paper if the space below is inadequate.

Author names:

This statement is signed by all the authors to indicate agreement that the above information is true and correct (*a photocopy of this form may be used if there are more than 10 authors*):

Author's name (typed)	Author's signature	Date
Hossein Haghighi	Hossein Haghighi	9.7.2019
Serge Kameni Leugoue		9.7.2019
Frank Pfeifer	Frank Pfeifer	23.07.2019
Heinz Wilhelm Siesler	H. W. Siesler	23.07.2019
Fabio Licciardello		09.07.2019
Patrizia Fava		09.07.2019
Andrea Pulvirenti		9.7.2019